JOURNAL OF NEUROTRAUMA 30:1092–1099 (June 15, 2013)

DOI: 10.1089/neu.2012.2728

Short Communication

Early Phrenic Motor Neuron Loss and Transient Respiratory Abnormalities after Unilateral Cervical Spinal Cord Contusion

Charles Nicaise,[1,2] David M. Frank,[1] Tamara J. Hala,[1] Michèle Authelet,[2] Roland Pochet,[2] Dominique Adriaens,[3] Jean-Pierre Brion,[2] Megan C. Wright,[4] and Angelo C. Lepore[1]

Abstract

Contusion-type cervical spinal cord injury (SCI) is one of the most common forms of SCI observed in patients. In particular, injuries targeting the C3–C5 region affect the pool of phrenic motor neurons (PhMNs) that innervates the diaphragm, resulting in significant and often chronic respiratory dysfunction. Using a previously described rat model of unilateral midcervical C4 contusion with the Infinite Horizon Impactor, we have characterized the early time course of PhMN degeneration and consequent respiratory deficits following injury, as this knowledge is important for designing relevant treatment strategies targeting protection and plasticity of PhMN circuitry. PhMN loss (48% of the ipsilateral pool) occurred almost entirely during the first 24 h post-injury, resulting in persistent phrenic nerve axonal degeneration and denervation at the diaphragm neuromuscular junction (NMJ). Reduced diaphragm compound muscle action potential amplitudes following phrenic nerve stimulation were observed as early as the first day post-injury (30% of pre-injury maximum amplitude), with slow functional improvement over time that was associated with partial reinnervation at the diaphragm NMJ. Consistent with ipsilateral diaphragmatic compromise, the injury resulted in rapid, yet only transient, changes in overall ventilatory parameters measured via whole-body plethysmography, including increased respiratory rate, decreased tidal volume, and decreased peak inspiratory flow. Despite significant ipsilateral PhMN loss, the respiratory system has the capacity to quickly compensate for partially impaired hemidiaphragm function, suggesting that C4 hemicontusion in rats is a model of SCI that manifests subacute respiratory abnormalities. Collectively, these findings demonstrate significant and persistent diaphragm compromise in a clinically relevant model of midcervical contusion SCI; however, the therapeutic window for PhMN protection is restricted to early time points post-injury. On the contrary, preventing loss of innervation by PhMNs and/or inducing plasticity in spared PhMN axons at the diaphragm NMJ are relevant long-term targets.

Key words: cervical; contusion; PhMN; rat; SCI

Introduction

More than half of traumatic spinal cord injury (SCI) cases occur in cervical spinal cord. Lesions targeting the C3–C5 midcervical region affect the phrenic nucleus that is composed of phrenic motor neuron (PhMN) cell bodies that innervate the diaphragm, a muscle centrally important to inspiration. Consequent breathing deficits depend upon severity and location of injury, varying from partial respiratory compromise to total dependence on mechanical ventilation. A major therapeutic target that needs to be evaluated in relevant SCI animal models is protection of PhMNs during the period of secondary degeneration following initial trauma.[1] We previously described a model of midcervical (C4) contusion in the adult rat.[2] We demonstrated that this paradigm models a number of the histopathological and functional features seen in human patients,[3,4] including extensive PhMN loss, phrenic nerve axonal degeneration, diaphragm atrophy, and chronically persistent unilateral diaphragm deficits, such as decreased diaphragm compound muscle action potential (CMAP) amplitudes following phrenic nerve stimulation, making it a clinically relevant model of respiratory compromise following midcervical contusion SCI. Nevertheless, experimental data are lacking regarding the timing of early PhMN loss and the consequent role of gray matter sparing on global breathing function during the initial stages

[1]Department of Neuroscience, Farber Institute for Neurosciences, Thomas Jefferson University Medical College, Philadelphia, Pennsylvania.
[2]Laboratory of General Histology, Neuroanatomy and Neuropathology, Université Libre de Bruxelles, Bruxelles, Belgium.
[3]Evolutionary Morphology of Vertebrates, Ghent University, Gent, Belgium.
[4]Department of Biology, Arcadia University, Glenside, Pennsylvania.

following midcervical spinal contusion.[5,6] Detailed characterization of the time course of PhMN loss post-injury will provide valuable information for determining the therapeutic window for targeting secondary PhMN degeneration. We therefore focused our study on the analysis of PhMNs during the first 2 weeks following midcervical C4 contusion SCI, including PhMN loss, anterograde degeneration along the phrenic nerve, and innervation changes at the diaphragm neuromuscular junctions. We correlated our histopathological findings with both diaphragmatic functional testing using phrenic nerve conduction studies and effects on global respiratory function using whole-body plethysmography (WBP).

Methods

Animals and surgical procedures

Following intraperitoneal injection of ketamine (100 mg/kg), xylazine (5 mg/kg), and acepromazine (2 mg/kg) to induce anesthesia, adult female Sprague–Dawley rats (225–275 g) received a C4 unilateral contusion (right-sided), as previously described.[2] Briefly, the dorsal skin and underlying muscle layers were incised along the midline between the spinous processes of C2 and T1 to expose the cervical region of the spinal cord. The dorsal muscle layers were retracted, and the paravertebral muscles overlying C3–C5 were removed. Following unilateral laminectomy on the right side at C4 level, rats were subjected to a single C4 spinal contusion injury using the Infinite Horizon Impactor (Precision Systems and Instrumentation, Lexington, KY). The full procedure included unilateral laminectomy on the right side, clamping of the spinous processes of C2 and T2 using toothed Adson forceps to stabilize the whole spinal column, raising of the 1.5 mm diameter impactor tip 2.5 mm above the dura, and contusion of the spinal cord (bathed in 0.9% sterile saline) at a force of 395 kD.

To specifically track the PhMN pool, 15 μL of 0.2% cholera toxin β (CTβ) conjugated to Alexa555, a monosynaptic retrograde axonal tracer, were delivered into the right intrapleural space 10 days prior to SCI, according to a modified protocol from Mantilla and colleagues.[2,7]

Experiments were conducted in compliance with the European Communities Council Directive (2010/63/EU, 86/609/EEC and 87-848/EEC), the National Institutes of Health (NIH) Guide for the Care and Use of Laboratory Animals, and the Thomas Jefferson University Institutional Animal Care and Use Committee (IACUC). Animals were monitored daily until euthanasia, from 1 to 14 days post-injury (DPI).

Experimental design

Twenty-nine animals were included in this study and were divided into five groups: injured animals killed at 1 DPI ($n=5$), 4 DPI ($n=9$), 8 DPI ($n=5$) or 14 DPI ($n=5$) and uninjured laminectomy-only controls killed at 14 DPI ($n=5$). All animals underwent WBP on a daily basis. Recordings of diaphragm compound muscle action potentials were terminal procedures conducted under anesthesia immediately before euthanasia.

WBP

WBP was used to quantify ventilation in unanesthetized spinally injured rats. Briefly, rats were exposed to normal air conditions in a plethysmography chamber (Buxco) for an hour of acclimation. Fresh air flow (rate = 2.5 L/min) was continuously provided to avoid CO_2 accumulation. The chamber temperature, pressure, and air flows were measured and integrated in the Drorbaugh and Fenn equation to calculate tidal volume, respiratory frequency, minute ventilation, and peak inspiratory flow.[8–10] Tidal volume and minute ventilation were further normalized to body weight. Recordings were averaged over 5 min once quiet breathing was reached.

Diaphragm CMAPs

Under anesthesia, supramaximal stimuli (0.5 ms duration; 6mV amplitude) were delivered through needle electrodes placed 0.5 cm apart along the right phrenic nerve, as previously described.[2] CMAP response was recorded via a surface strip along the costal margin of the right hemidiaphragm. Peak-to-peak amplitudes of CMAPs from 10 stimulations were recorded to assess intra-animal variability and confirm reproducibility.

Histology

At euthanasia, rats were deeply anesthetized and transcardially perfused with 0.9% NaCl, followed by 4% buffered paraformaldehyde. Cervical spinal cord, phrenic nerves, and diaphragm were then removed. Cryostat 30 μm spinal cord sections were processed for standard Nissl/Eriochrome R staining to quantify lesion size and motor neuron loss, as previously described.[2,11] Three-dimensional (3-D) reconstruction of the injured cervical spinal cord was performed on serial histological sections using Free-D software, according to developer instructions.[12] Large Nissl$^+$ motor neurons with a soma size $> 200\ \mu m^2$ and a clearly visible nucleolus were counted in the ipsilateral ventral horn. Number of total motor neurons per ipsilateral ventral horn was plotted at specific distances relative to lesion epicenter. Lesion epicenter was defined as the section with the largest percent lesioned tissue (relative to total tissue area in the same section). To visualize and estimate total numbers of CTβ^+ PhMNs, spinal cord sections were mounted with fluorescence-compatible reagent. Numbers of CTβ^+ cells per ipsilateral ventral horn were analyzed and plotted at specific distances relative to the lesion epicenter.

Phrenic nerves were fixed in 4% glutaraldehyde, post-fixed in 2% (w/v) OsO_4 for 30 min, dehydrated, and embedded in Epoxy resin LX112. Semi-thin cross sections (1–2 μm) were cut and stained with Toluidine blue 1%. The number of myelinated axons per unit area was assessed using ImageJ software, as previously reported.[2]

Hemidiaphragm muscle was dissected from each animal for whole-mount immunohistochemistry, as previously described.[2,13] Motor axons and their presynaptic terminals were labeled with SMI-312R (Covance) and SV2-s (Developmental Studies Hybridoma Bank [DSHB]), respectively, and both labelings were detected with FITC anti-mouse Immunoglobulin G (IgG) secondary (Jackson ImmunoResearch). Postsynaptic acetylcholine receptors were labeled with Alexa Fluor 647-conjugated α-bungarotoxin (Invitrogen). Labeled muscles were analyzed for total numbers of neuromuscular junctions (NMJs), and were further categorized as: ''intact'' NMJs with full overlapping of pre- and postsynaptic domains, denervated NMJs (partial or complete), and NMJs with signs of reinnervation.[13]

Statistical analyses

Significance was assessed by analysis of variance (one-way ANOVA), followed by multiple comparisons post-hoc test (Bonferroni's method) for multiple comparisons. $P < 0.05$ was considered as significant.

Results

As early as 1 DPI, contusion altered the general structure of gray matter, producing a striking loss of Nissl$^+$ neurons. In white matter, the lesion extended to dorsolateral, lateral, and ventrolateral funiculi (Fig. 1A). Signs of hemorrhage (arrowheads in Fig. 1A) were detectable along with significant swelling of the injured hemicord. Lesion size expanded over time, increasing at lesion epicenter from 45% of ipsilateral hemicord at 1 DPI to 69% at 14 DPI (Fig. 1B). Overall lesion volume significantly changed between 1 and 14 DPI,

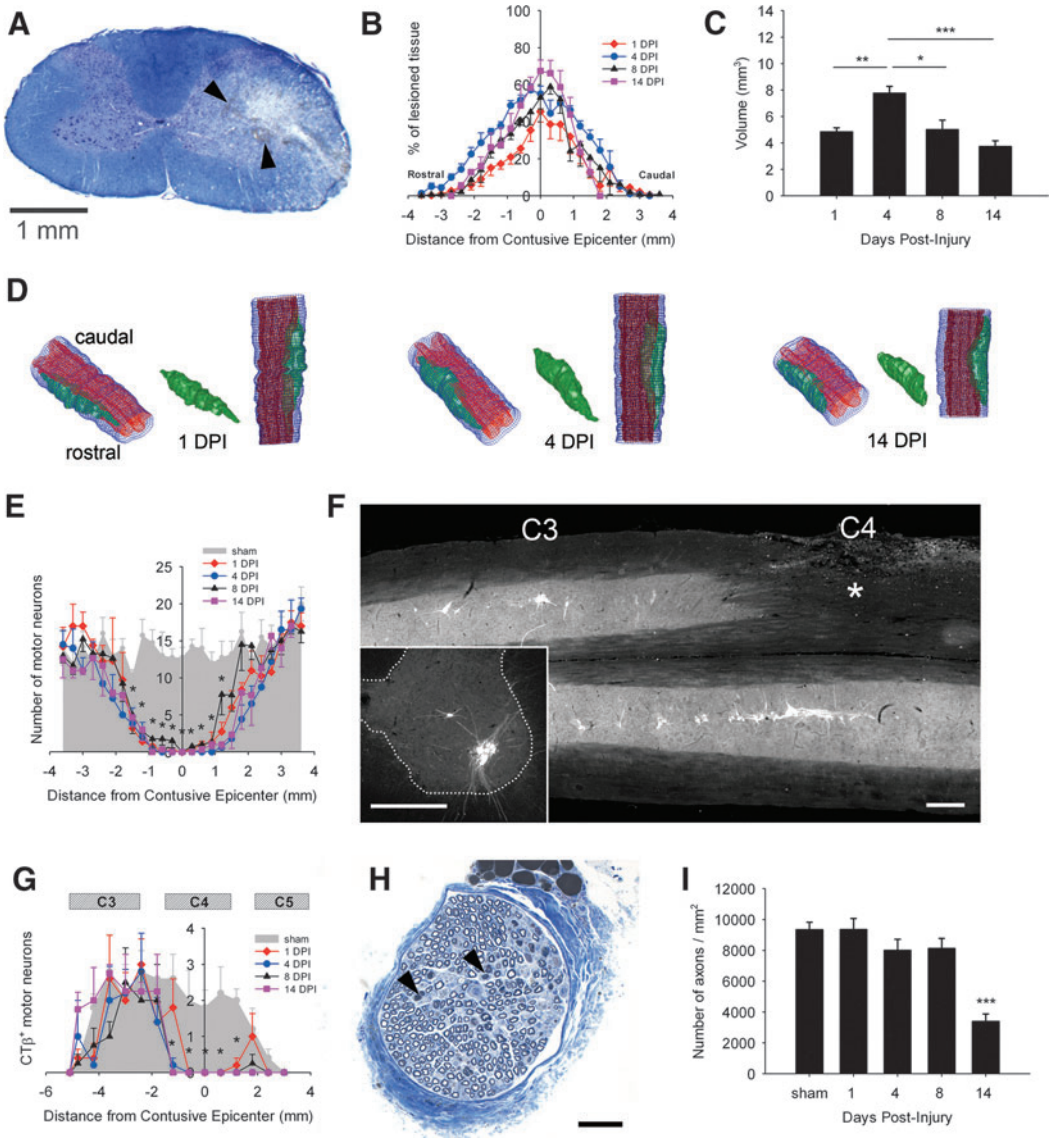

FIG. 1. Early time course of histopathology following unilateral C4 cervical contusion. Eriochrome R/Nissl staining shows the lesion epicenter at 1 day post-injury (DPI) **(A)**. Evidence of hemorrhage and edema is observed in ipsilesioned hemicord (arrowheads in **A**). Loss of large Nissl$^+$ motor neurons in ipsilateral ventral horn was observed in addition to white matter disruption in dorsolateral, lateral and ventrolateral funiculi (scale bar: 1mm). The lesion size expanded over time, particularly at the epicenter **(B)**. There was a significant increase in total lesion volume at 4 DPI, likely because of spinal cord swelling **(C)**. Three-dimensional (3-D) reconstruction of the cervical spinal cord shows that the injury damaged both gray and white matter **(D)**. At 1 DPI, there was significant extension of the lesion in rostral and caudal directions from the epicenter. At 14 DPI, there was still significant rostral-caudal extension; however, the lesion became more concentrated to the contusion epicenter (blue: entire spinal cord; red: gray matter; green: lesion). After C4 injury, a significant loss of motor neurons over a rostral-caudal length of ~ 4 mm was observed surrounding the lesion epicenter **(E)**. There were no differences among all time points from 1 to 14 DPI. The phrenic motor neuron (PhMN) pool was specifically labeled with cholera toxin β (CTβ)-Alexa555 via retrograde tracing from the diaphragm. CTβ^+ PhMNs were identified in the area of the phrenic nucleus: mid-C3 to the rostral part of C5 **(F)**. Representative illustrations show a longitudinal section of the phrenic nucleus following C4 injury (asterisk in **F**) and a transverse section from an uninjured control animal (Inset in **F**). Bars represent 500 μm in **F**. Numbers of CTβ^+ PhMNs were quantified in transverse sections (inset in **F**). In the ipsilesioned hemicord, there was a significant loss of CTβ^+ PhMNs at multiple distances from the lesion epicenter compared with injured controls **(G)** at 600 μm rostral, at epicenter, at 600 μm caudal, and up to 1200 μm caudal. Compared with 1 DPI, additional PhMN loss occurred rostrally at 1200 μm at 4 DPI, 8 DPI, and 14 DPI. As early as 4 DPI, phrenic nerves from C4 injured animals exhibited histopathological changes such as degenerating fibers (arrowheads in **H**). Bar represents 50 μm in **H**. Axonal density (i.e., number of myelinated fibers per unit area) was significantly decreased at 14 DPI compared with the uninjured group **(I)**. Results are expressed as means $\pm$ SEM. Statistical significance was assessed by analysis of variance (one-way ANOVA) and multiple comparisons post-hoc test (Bonferroni's method). *DPI versus uninjured ($p < 0.05$); **DPI versus uninjured ($p < 0.01$); ***DPI versus uninjured ($p < 0.001$). $n = 5$ animals for uninjured group and for injured animals at 1, 8, and 14 DPI; $n = 9$ animals for injured animals at 4 DPI. Color image is available online at www.liebertpub.com/neu

reaching its maximal size at 4 DPI (7.7 ± 0.5 vs. $4.8 \pm 0.3\,mm^3$, $p < 0.01$ compared with 1 DPI). This larger volume at 4 DPI was likely because of the presence of edema, which progressively resolved over time (Fig. 1C). 3-D modeling of the injury shows spreading of the lesion in white and gray matter (Fig. 1D). Marked differences in lesion volume between early time points (i.e., 1 DPI, 4 DPI) and 14 DPI may be explained by the resolution of hemorrhage and edema in the cord. In particular, the lateral funiculus was one of the most affected spinal regions along the lesion length in our paradigm (Supplementary Videos 1, 2 and 3: 1 DPI, 4 DPI, 14 DPI, respectively) (see online supplementary material at http://www.liebertpub.com/neu).

Large $Nissl^+$ motor neurons meeting our size criterion ($> 200\,\mu m^2$) were counted in the ipsilateral ventral horn. Compared with laminectomy-only control group, C4 injured rats showed significant motor neuron loss at multiple distances from epicenter at all time points (Fig. 1E). To specifically track PhMN survival, fluorescent CTβ was delivered into the intrapleural space. CTβ^+ PhMNs were arranged along a linear column extending from mid-C3 to rostral C5. As shown in Figure 1F, unilateral injury (asterisk) disrupted gray matter integrity and induced obvious loss of CTβ^+ PhMNs. PhMNs were quantified in transverse sections from injured and control rats (inset in Fig. 1F). C4 injured rats showed a significant loss of CTβ^+ PhMNs at multiple distances surrounding the lesion epicenter (Fig. 1G): 600 μm rostral ($p < 0.05$, all DPI vs. uninjured), epicenter ($p < 0.001$, all DPI vs. uninjured), 600μm caudal ($p < 0.01$, all DPI vs. uninjured), and up to 1200 μm caudal ($p < 0.001$, all DPI vs. uninjured). Compared with 1 DPI, additional PhMN loss occurred rostrally at 1200 μm at 4 DPI ($p < 0.05$), 8 DPI ($p < 0.01$), and 14 DPI ($p < 0.01$). From this analysis, we estimated the percentage of total spared PhMNs in ipsi-lesioned phrenic nucleus to be 52% at 1 DPI, with a nonsignificant decrease to 48% by 14 DPI, most of them located rostral to C4.

We further assessed anterograde degeneration of the ipsilateral phrenic nerve in toluidin blue stained semi-thin sections. Although not significant, a slight decrease in phrenic nerve axonal counts was detected at 4 DPI, which was supported by histological findings of sparse Wallerian degeneration and axonal shrinkage (arrowheads in Fig. 1H). Axonal density was statistically decreased by 64% (3400 ± 484 vs. 9344 ± 491 axons/mm^2, $p < 0.001$) at 14 DPI compared with uninjured controls (Fig. 1I). Given the early loss of PhMNs, we characterized the impact on diaphragm innervation by performing a time course analysis of the diaphragm NMJ. Motor axons and their terminals were labeled for neurofilament (SMI-312) and synaptic vesicles (SV-2), respectively, and postsynaptic acetylcholine receptors were labeled with rhodamine-conjugated α-bungarotoxin. Uninjured hemidiaphragms showed typical morphology of intact NMJs, including thick pre-terminal axons and

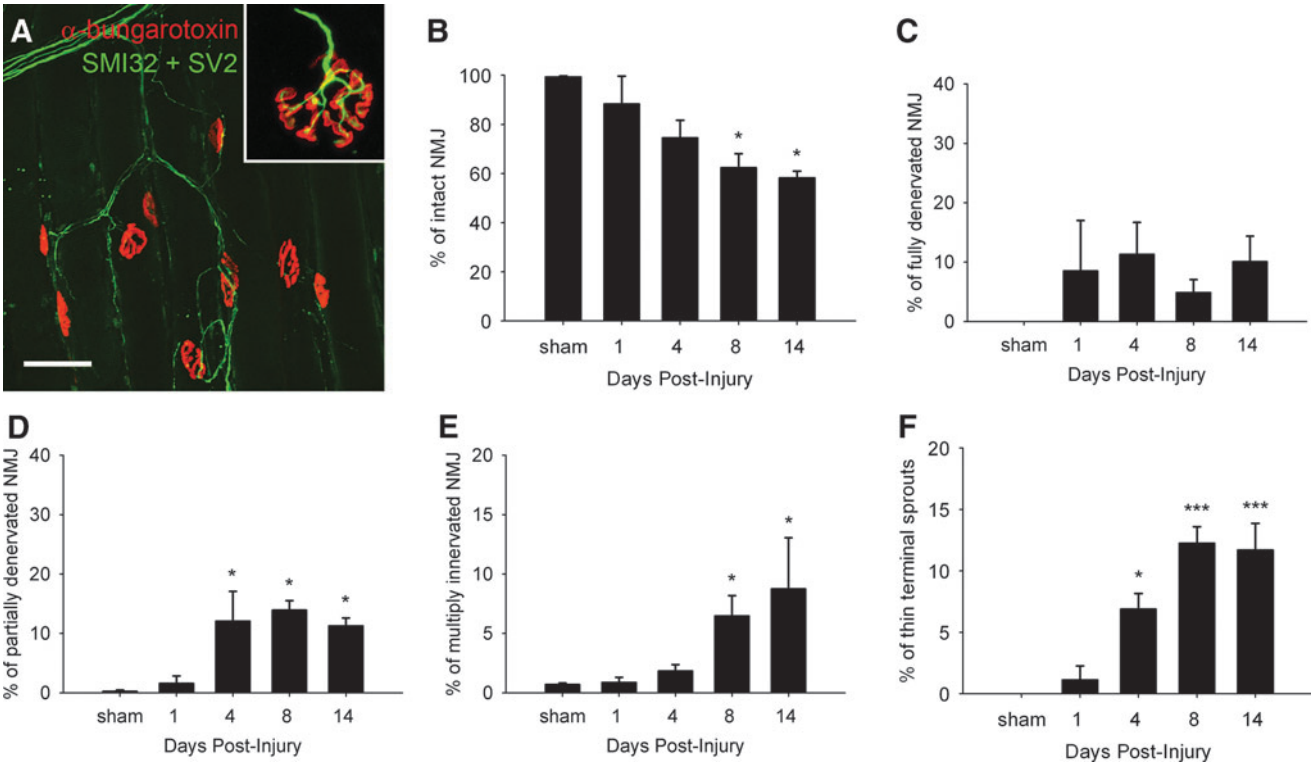

FIG. 2. Morphological changes at the diaphragm neuromuscular junction (NMJ)**.** Diaphragm neuromuscular junctions (NMJs) were assessed via labeling with rhodamine-α-bungarotoxin (red), SMI-312R (green) and SV2-s (green). All NMJs were completely intact in uninjured control rats, characterized by complete overlap of the presynaptic axon and presynaptic vesicles with postsynaptic acetylcholine receptors (Inset in **A**). Bar represents 50 μm in **A**. Following injury **(A)**, the number of intact NMJs progressively decreased, reaching significance at 8 days post-injury (DPI) and 14 DPI **(B)**. A significant portion of the abnormal junctions at 4, 8, and 14 DPI were categorized as partially denervated (**D**), although the presence of fully denervated NMJs was also observed at these time points (**C**). Signs of reinnervation, supported by the presence of multiply innervated NMJS **(E)** and thin axonal terminal sprouts **(F)**, were detected as early as 4 DPI. Results are expressed as means $\pm$ SEM. Statistical significance was assessed by analysis of variance (one-way ANOVA) and multiple comparisons post-hoc test (Bonferroni's method). *DPI versus uninjured ($p < 0.05$); ***DPI versus uninjured ($p < 0.001$). $n = 3$ animals per group for all groups. Color image is available online at www.liebertpub.com/neu

complete overlap of pre- and postsynaptic domains (Inset in Fig. 2A). Whereas uninjured rats exhibited fully intact NMJs, injured rats showed signs of progressive synaptic disruption, with the percentage of intact junctions declining to 88% (p = ns), 74% (p = ns), 62% ($p < 0.05$), and 58% ($p < 0.05$) at 1, 4, 8, and 14 DPI, respectively (Fig. 2B). Early NMJ abnormalities, such as complete or partial denervation, were detected in the ipsilateral hemidiaphragm (Fig. 2A). A significant portion of the abnormal junctions at 4, 8, and 14 DPI were categorized as partially denervated (Fig. 2D), although the presence of fully denervated NMJs was also observed at these time points (Fig. 2C). Similar to our previous reports, we have observed differential degrees of denervation at various dorsal-ventral subregions of the hemidiaphragm muscle. These effects were the result of topographical diaphragm innervation that coincides with the rostral-caudal position of PhMNs within the cervical spinal cord.[2,14] Interestingly, as early as 4 DPI, significant numbers of NMJs exhibiting profiles of multiple innervation (Fig. 2E) or thin pre-terminal axonal sprouts (Fig. 2F), characteristic signs of reinnervation at the NMJ, were observed. The occurrence of these thin pre-terminal axonal sprouts, for example, strikingly increased over time, from 1.1% at 1 DPI to 11.7% of total NMJs at 14 DPI ($p < 0.001$) .

To correlate these pathohistological events with potential respiratory compromise, we investigated ipsilateral hemidiaphragm function and overall respiratory function by conducting phrenic nerve conduction studies and repeated unrestrained WBP, respectively. CMAP responses in uninjured rats reached ~7.3mV (7.3 ± 0.4mV) (Fig. 3B), whereas amplitudes were reduced in injured animals (Fig. 3C). Compared with the uninjured group, CMAP amplitudes were reduced at 1 DPI (2.5 ± 0.2 mV, $p < 0.001$) and 4 DPI (2.1 ± 0.3 mV, $p < 0.01$), followed by partial improvement at 8 (3.8 ± 0.5 mV) and 14 DPI (4.2 ± 0.3 mV) (Fig. 3A). Regarding ventilation, respiratory changes were only transient (Fig. 3D–H). Significantly elevated respiratory rate was observed in injured animals at 1 DPI (91.9 ± 5.6 vs. 65.7 ± 3.5 bpm, $p < 0.01$), whereas tidal volume (0.62 ± 0.02 vs. 0.84 ± 0.02 mL/breath, $p < 0.001$) and peak inspiratory flow (8.1 ± 0.9 vs. 12.9 ± 1.2 mL/sec, $p < 0.01$) were both reduced at 1 DPI compared with the uninjured

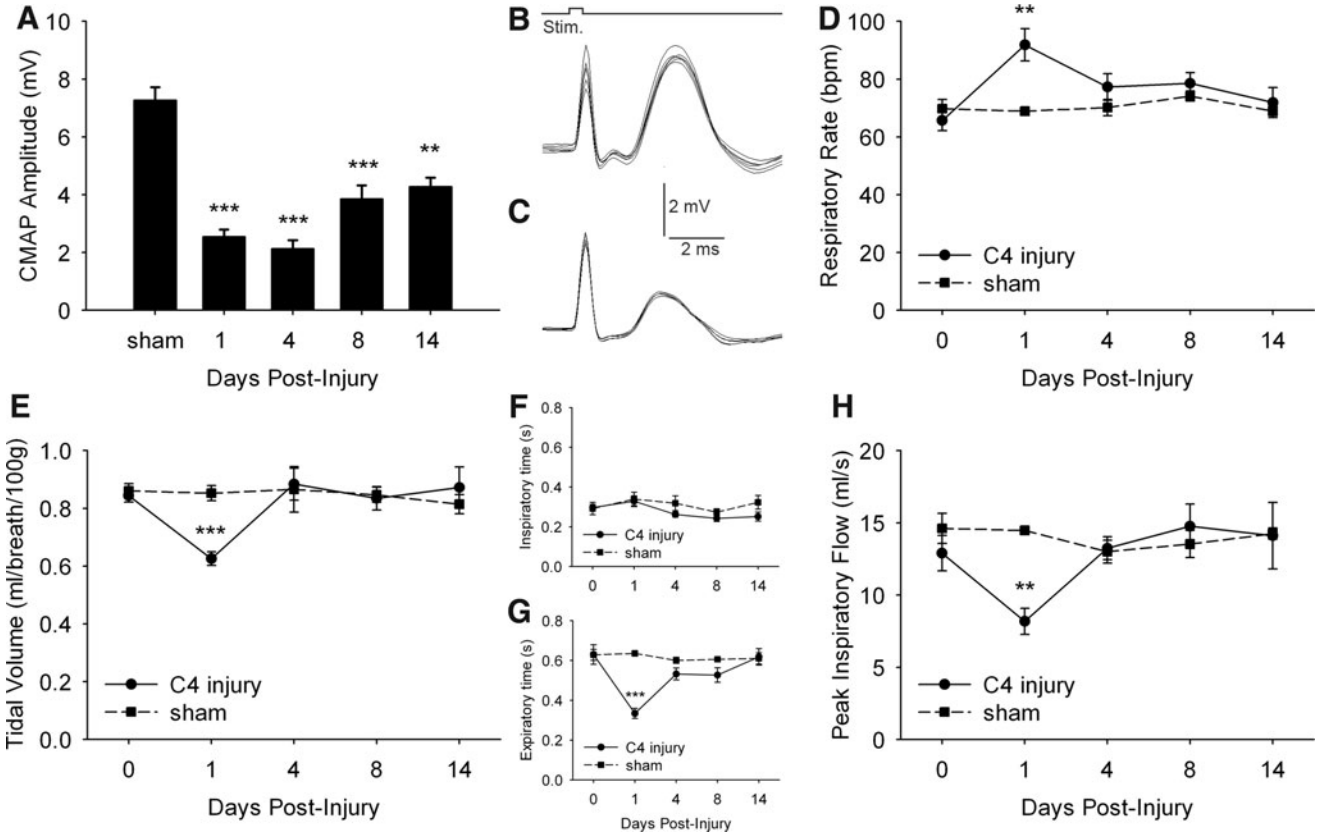

FIG. 3. Time course of diaphragm compound muscle action potentials (CMAPs) and ventilatory parameters using whole-body plethysmography following unilateral C4 cervical contusion. Compared with laminectomy-only uninjured animals **(B)**, C4 injured rats **(C)** had reduced CMAP amplitudes in ipsilateral hemidiaphragm following phrenic nerve stimulation, a functional electrophysiological assay of phrenic motor neuron (PhMN) innervation of the diaphragm. Significantly decreased peak CMAP amplitudes were observed at all time points post-injury, with a trend toward improvement at 8 and 14 days post-injury (DPI) **(A)**. Using whole-body plethysmography, respiratory rate **(D)**, tidal volume **(E)**, inspiratory and expiratory duration **(F,G),** and peak inspiratory flow **(H)** were determined under normoxic conditions repeatedly on the same animals before and after spinal cord injury (SCI). Respiratory rate significantly increased at 1 DPI in injured rats compared to uninjured controls and returned to pre-injury baseline at 4, 8 and 14 DPI **(D)**. Similarly, significant changes in tidal volume **(E)**, expiratory time **(G)** and peak inspiratory flow **(H)** were transient in injured rats, with differences observed only at 1 DPI. No differences were measured for inspiratory time **(F)** or minute ventilation (not shown). Results are expressed as means ± SEM. Statistical significance was assessed by analysis of variance (one-way ANOVA) and multiple comparisons post-hoc test (Bonferroni's method). **DPI versus uninjured ($p < 0.01$); ***DPI versus uninjured ($p < 0.001$). $n = 5$ animals for uninjured group and for injured animals at 1, 8, and 14 DPI; $n = 9$ animals for injured animals at 4 DPI.

group (Fig. 3D, E, H). Minute ventilation did not change over time (data not shown). The increased respiratory rate was likely the result of the shortened duration of expiration (0.33 ± 0.02 vs. 0.63 ± 0.05 sec, $p < 0.001$, C4 injury vs. uninjured), as duration of inspiration was unchanged (Fig. 3F–G). At all time points examined after 1 DPI, no differences in any breathing parameters were observed between uninjured and contusion groups.

Discussion

In order to develop therapies targeting clinically important outcomes relevant to respiratory compromise following cervical SCI, we sought to characterize the time course of PhMN loss and diaphragmatic dysfunction in a rat model of unilateral contusion SCI that targets the phrenic nucleus. Few studies have characterized the pathologic events taking place at the phrenic nucleus following contusion SCI. For example, using WBP, Golder and colleagues demonstrated that a single midcervical contusion injury modified the general ventilator response over a short time frame (i.e., 2 DPI).[9] In a similar injury paradigm, Lane and colleagues extended these investigations by showing that diaphragm activity was chronically impaired following a bilateral midcervical contusion injury; however, general ventilatory parameters were unaffected.[10]

Our study demonstrates that following unilateral C4 contusion SCI, PhMN loss in the ipsilateral phrenic nucleus primarily occurs within the first 24 h post-injury. Very early loss of motor neurons (i.e., between 12 and 24 h post-injury) has already been shown in thoracic contusion models,[15–17] further suggesting that therapeutic interventions targeting motor neuron sparing should be delivered within 1 DPI. Surprisingly, only a small extension of PhMN loss was observed over time, despite the progressive increase in lesion volume beyond 1 DPI. Consistent with our observations and other work,[2,15] Andrade and colleagues showed that secondary neurodegeneration is pronounced following moderate SCI, unlike following more severe injury.[18] In our current study, the secondary degenerative process may have been minimized because of the severity of the initial 395 kD impact. In the present study, we examined overt PhMN loss caused by necrosis. However, other injury-related effects on respiratory neuron circuitry, such as damage to spared PhMNs, disruption of descending bulbospinal axons, and compromise in synaptic connections between these supraspinal neurons and spared PhMNs of the cervical spinal cord were not analyzed, and warrant further investigation, as they may be involved in pathophysiological outcomes.

We first observed peripheral histological abnormalities at 4 DPI, with denervation at the diaphragm NMJ occurring earlier than overt phrenic nerve axonal loss. Despite the progressive axonal loss that occurred in the phrenic nerve, we observed reinnervation of diaphragm NMJs as early as 4 DPI. In our current analysis, we have presented the percentage of denervation across the entire hemidiaphragm, thereby underestimating the changes seen at highly affected regions of the muscle. In most instances of our quantitative NMJ analysis, the fibers of the multiply innervated NMJs could be visually traced back to remaining adjacent intact NMJs or regenerating nerve fibers in the denervated nerve bundles within the hemidiaphragm ipsilateral to the injury. Combined with work by Mantilla and colleagues showing that rat hemidiaphragm is only innervated by ispilateral PhMNs, these findings suggest that neurite sprouting/regenerating fibers originated from PhMN axons ipsilateral to the hemicontusion. Characterizing peripheral changes such as reinnervation after midcervical injuries will result in a better understanding of the events involved in recovery of motor nerve function and consequent respiratory performance. For example, this process may have accounted for the delayed recovery in ipsilateral CMAP amplitudes at 8 and 14 DPI. Strakowski and colleagues described a slight recovery of CMAP amplitude in patients with cervical SCI that occurred over a period of months. This spontaneous CMAP improvement was associated with successful weaning off of mechanical ventilation,[3] emphasizing the usefulness of phrenic nerve studies for understanding functional breathing recovery.[19] The improvement in CMAP responses that we have observed in the current study might also be linked to the resolution of hemorrhage and edema in the spinal cord and/or ventral root, which is observed in the initial days following human SCI.[4] Restoration of the blood–brain barrier and extracellular ion and neurotransmitter homeostasis may also play important roles. However, in our rat cervical contusion model, we previously showed that CMAPs remain chronically reduced for at least 6 weeks, suggesting that these early events only account for partial CMAP loss.[2] Collectively, these findings suggest that manipulation of phrenic nerve–diaphragm connectivity may be a valuable target for maintaining diaphragm function at later time points following cervical SCI, especially given the limited early time window for protecting PhMNs.

Progressive spontaneous recovery of diaphragm activity may occur through phrenic nerve sprouting and/or bulbospinal pathway reorganization. Reinnervation at the denervated hemidiaphragm NMJ can be achieved via sprouting from spared ipsilateral PhMNs (i.e., located at the C3 level in our C4 injury paradigm), as we have demonstrated in the present study. Spared or previously silent C3 PhMNs can also be recruited in an effort to maintain or enhance effective diaphragm contraction.[10] This hypothesis was supported by findings from el-Bohy and colleagues that demonstrated an increase in phrenic neurogram activity ipsilateral to contusion.[5] In our previous study, we found an increase in hemidiaphragm EMG activity ipsilateral to the cervical injury site,[2] supporting the notion of increased drive from supraspinal circuitry. Local changes in spinal circuits or reorganization of suprapinal pathways have been extensively described following C2 hemisection;[19–21] however, at present we are uncertain of the effect of a midcervical contusion injury on these mechanisms. Neuronal mechanisms underlying spontaneous CMAP recovery remain largely unknown, but might involve the crossed-phrenic pathway, plasticity of pre-phrenic interneurons, recruitment of spared PhMNs or new motor units, and changes in PhMN excitability via alterations in expression of glutamatergic and/or serotoninergic receptors. Characterization of these potential recovery mechanisms deserves further investigation in cervical contusion paradigms. Although one could argue that contusion injuries are more clinically relevant than cervical hemisection, these injuries are challenging in terms of pathophysiology, as they present the complication of disrupting both local gray and white matter and descending axonal input to gray matter at and below the lesion.

We have demonstrated that persistent ipsilateral hemidiaphragm deficits were associated with only transient impairment in overall ventilatory parameters, similar to effects observed in some cases of human SCI.[22,23] Our findings are in accordance with experimental data previously reported in unilateral C5 contusion[8] and bilateral cervical contusion[9,10] paradigms. Most of these studies demonstrated transient changes in respiratory rate and tidal volume under normoxic conditions, but no effects on global minute ventilation. At 1 DPI, our spinally injured rats exhibited a reduced tidal volume, and they had a higher respiratory rate to maintain the same minute

ventilation as control animals. Under quiet breathing, minute ventilation of injured rats is not distinguishable from that of uninjured rats; however, this might not be the case with respiratory challenge. A limitation of our study is the recording of ventilatory patterns only under normoxic conditions. It has been demonstrated that respiratory abnormalities could be detected up to 4 weeks following C5 SCI under hypercapnic conditions (although this response ultimately recovered), whereas under normocapnia, the abnormality only lasted for 2 weeks.[8] Collectively, these data suggest that animal models of midcervical hemicontusion manifest subacute respiratory abnormalities. To date, none of the existing cervical contusion SCI models are able to induce persistent ventilatory deficits during both resting breathing and respiratory challenge.[8–10] As suggested by Lane and colleagues from a translational point of view,[10] current cervical contusion paradigms seem to model incomplete cervical SCI (as defined by the American Spinal Injury Association [ASIA] Impairment Scale) or SCI patients weaned from mechanical ventilation, as breathing deficits are observed when the cardiorespiratory system is challenged (i.e., during exercise or hypercapnia).[24–28]

A noteworthy ventilatory parameter is peak inspiratory flow, which reflects inspiratory muscle strength in the absence of airway pathology.[29] In our injury model, inspiratory flow was reduced during the first 24 h post-contusion, suggesting temporary compromise in inspiratory muscle function. It is likely that compensation from contralateral unaffected hemidiaphragm and/or accessory inspiratory muscles allowed for rapid recovery to basal levels. Parallel compensatory mechanisms involving nonphrenic respiratory pathways such as expiratory muscles may have also led to recovery, as well as to the increased respiratory rate observed at 1 DPI. Taken together, these data suggest that the respiratory system has the ability to quickly compensate for unilateral diaphragm deficits by modifying both inspiratory and expiratory breathing patterns.

The time course of histopathological and functional changes following our unilateral C4 contusion provides a number of insights for defining therapeutic windows. This injury paradigm also provides a useful model for assessing the potential benefits of various treatment strategies, such as molecular therapies, pharmacological intervention, and cell transplantation. Cell replacement, neuroprotection, and induction of plasticity in white matter locations following cervical SCI are prominent strategies for targeting respiratory neural pathways. Encouragingly, promising results showing that gray matter repair can also influence PhMN function and circuitry following cervical SCI, are beginning to emphasize the importance of gray matter-based interventions, including PhMN protection.[6,30]

Acknowledgments

This work was supported by the Université Libre de Bruxelles (Bureau des Relations Internationales et de la Coopération, grant BRIC-11/092 to Dr. Nicaise), the Craig Nielsen Foundation (C.N.F. grant #190140 to Dr. Lepore), and the National Institute of Neurological Disorders and Stroke (NINDS) (R01 grant to Dr. Lepore). We thank Emmanuel Gilissen, Céline Neutens, and Mathias Bouilliart for support with 3D reconstruction. We thank Amir Pelleg and Kiarash Emami for valuable advice in setting up the WBP.

Author Disclosure Statement

No competing financial interests exist.

References

1. Sharma, H., Alilain, W.J., Sadhu, A., and Silver, J. (2012). Treatments to restore respiratory function after spinal cord injury and their implications for regeneration, plasticity and adaptation. Exp. Neurol. 235, 18–25.
2. Nicaise, C., Hala, T.J., Frank, D.M., Parker, J.L., Authelet, M., Leroy, K., Brion, J.P., Wright, M.C., and Lepore, A.C. (2012). Phrenic motor neuron degeneration compromises phrenic axonal circuitry and diaphragm activity in a unilateral cervical contusion model of spinal cord injury. Exp. Neurol. 235, 539–552.
3. Strakowski, J.A., Pease, W.S., and Johnson, E.W. (2007). Phrenic nerve stimulation in the evaluation of ventilator-dependent individuals with C4- and C5-level spinal cord injury. Am. J. Phys. Med. Rehabil. 86, 153–157.
4. Norenberg, M.D., Smith, J., and Marcillo, A. (2004). The pathology of human spinal cord injury: defining the problems. J. Neurotrauma 21, 429–440.
5. el-Bohy, A.A., Schrimsher, G.W., Reier, P.J., and Goshgarian, H.G. (1998). Quantitative assessment of respiratory function following contusion injury of the cervical spinal cord. Exp. Neurol. 150, 143–152.
6. Reier, P.J., Golder, F.J., Bolser, D.C., Hubscher, C., Johnson, R., Schrimsher, G.W., and Velardo, M.J. (2002). Gray matter repair in the cervical spinal cord. Prog. Brain Res. 137, 49–70.
7. Mantilla, C.B., Zhan, W.Z., and Sieck, G.C. (2009). Retrograde labeling of phrenic motoneurons by intrapleural injection. J. Neurosci. Methods 182, 244–249.
8. Choi, H., Liao, W.L., Newton, K.M., Onario, R.C., King, A.M., Desilets, F.C., Woodard, E.J., Eichler, M.E., Frontera, W.R., Sabharwal, S., and Teng, Y.D. (2005). Respiratory abnormalities resulting from midcervical spinal cord injury and their reversal by serotonin 1A agonists in conscious rats. J. Neurosci. 25, 4550–4559.
9. Golder, F.J., Fuller, D.D., Lovett–Barr, M.R., Vinit, S., Resnick, D.K., and Mitchell, G.S. (2011). Breathing patterns after mid-cervical spinal contusion in rats. Exp. Neurol. 231, 97–103.
10. Lane, M.A., Lee, K.Z., Salazar, K., O'Steen, B.E., Bloom, D.C., Fuller, D.D., and Reier, P.J. (2012). Respiratory function following bilateral mid-cervical contusion injury in the adult rat. Exp. Neurol. 235, 197–210.
11. Lepore, A.C., Rauck, B., Dejea, C., Pardo, A.C., Rao, M.S., Rothstein, J.D., and Maragakis, N.J. (2008). Focal transplantation-based astrocyte replacement is neuroprotective in a model of motor neuron disease. Nat. Neurosci. 11, 1294–1301.
12. Andrey, P., and Maurin, Y. (2005). Free-D: an integrated environment for three-dimensional reconstruction from serial sections. J. Neurosci. Methods 145, 233–244.
13. Wright, M.C., and Son, Y.J. (2007). Ciliary neurotrophic factor is not required for terminal sprouting and compensatory reinnervation of neuromuscular synapses: re-evaluation of CNTF null mice. Exp. Neurol. 205, 437–448.
14. Nicaise, C., Putatunda, R., Hala, T.J., Regan, K.A., Frank, D.M., Brion, J.P., Leroy, K., Pochet, R., Wright, M.C., and Lepore, A.C. (2012). Degeneration of phrenic motor neurons induces long-term diaphragm deficits following mid-cervical spinal contusion in mice. J. Neurotrauma 29, 2748–2760.
15. Min, K.J., Jeong, H.K., Kim, B., Hwang, D.H., Shin, H.Y., Nguyen, A.T., Kim, J.H., Jou, I., Kim, B.G., and Joe, E.H. (2012). Spatial and temporal correlation in progressive degeneration of neurons and astrocytes in contusion-induced spinal cord injury. J. Neuroinflammation 9, 100.
16. Teng, Y.D., Mocchetti, I., and Wrathall, J.R. (1998). Basic and acidic fibroblast growth factors protect spinal motor neurones in vivo after experimental spinal cord injury. Eur. J. Neurosci. 10, 798–802.
17. Grossman, S.D., Rosenberg, L.J., and Wrathall, J.R. (2001). Temporal-spatial pattern of acute neuronal and glial loss after spinal cord contusion. Exp. Neurol. 168, 273–282.
18. Andrade, M.S., Hanania, F.R., Daci, K., Leme, R.J., and Chadi, G. (2008). Contuse lesion of the rat spinal cord of moderate intensity leads to a higher time-dependent secondary neurodegeneration than severe one. An open-window for experimental neuroprotective interventions. Tissue Cell 40, 143–156.
19. El-Bohy, A.A., and Goshgarian, H.G. (1999). The use of single phrenic axon recordings to assess diaphragm recovery after cervical spinal cord injury. Exp. Neurol. 156, 172–179.

20. Vinit, S., Gauthier, P., Stamegna, J.C., and Kastner, A. (2006). High cervical lateral spinal cord injury results in long-term ipsilateral hemidiaphragm paralysis. J. Neurotrauma 23, 1137–1146.
21. Vinit, S., and Kastner, A. (2009). Descending bulbospinal pathways and recovery of respiratory motor function following spinal cord injury. Respir. Physiol. Neurobiol. 169, 115–122.
22. Loveridge, B., Sanii, R., and Dubo, H.I. (1992). Breathing pattern adjustments during the first year following cervical spinal cord injury. Paraplegia 30, 479–488.
23. Bluechardt, M.H., Wiens, M., Thomas, S.G., and Plyley, M.J. (1992). Repeated measurements of pulmonary function following spinal cord injury. Paraplegia 30, 768–774.
24. Higuchi, Y., Kitamura, S., Kawashima, N., Nakazawa, K., Iwaya, T., and Yamasaki, M. (2006). Cardiorespiratory responses during passive walking-like exercise in quadriplegics. Spinal Cord 44, 480–486.
25. Kelling, J.S., DiMarco, A.F., Gottfried, S.B., and Altose, M.D. (1985). Respiratory responses to ventilatory loading following low cervical spinal cord injury. J. Appl. Physiol. 59, 1752–1756.
26. Lin, K.H., Wu, H.D., Chang, C.W., Wang, T.G., and Wang, Y.H. (1998). Ventilatory and mouth occlusion pressure responses to hypercapnia in chronic tetraplegia. Arch. Phys. Med. Rehabil. 79, 795–799.
27. Manning, H.L., Brown, R., Scharf, S.M., Leith, D.E., Weiss, J.W., Weinberger, S.E., and Schwartzstein, R.M. (1992). Ventilatory and P0.1 response to hypercapnia in quadriplegia. Respir. Physiol. 89, 97–112.
28. Hopman, M.T., van der Woude, L.H., Dallmeijer, A.J., Snoek, G., and Folgering, H.T. (1997). Respiratory muscle strength and endurance in individuals with tetraplegia. Spinal Cord 35, 104–108.
29. West, C.R., Campbell, I.G., and Romer, L.M. (2012). Assessment of pulmonary restriction in cervical spinal cord injury: a preliminary report. Arch. Phys. Med. Rehabil. 93, 1463–1465.
30. White, T.E., Lane, M.A., Sandhu, M.S., O'Steen, B.E., Fuller, D.D., and Reier, P.J. (2010). Neuronal progenitor transplantation and respiratory outcomes following upper cervical spinal cord injury in adult rats. Exp. Neurol. 225, 231–236.

Address correspondence to:
Angelo C. Lepore, PhD
Department of Neuroscience
Farber Institute for Neurosciences
Thomas Jefferson University Medical College
900 Walnut Street, JHN 469
Philadelphia, PA 19107

E-mail: Angelo.Lepore@jefferson.edu